https://doi.org/10.17221/48/2025-VETMED

Impact of histological and molecular subtype on the potential therapeutic effect of buparlisib in canine mammary gland tumours

*Aslihan Baykal Ugur[1], Gamze Guney Eskiler[2], Ozge Turna[1]**

[1]*Department of Obstetrics and Gynecology, Faculty of Veterinary Medicine, Istanbul University-Cerrahpasa, Istanbul, Turkiye*
[2]*Department of Medical Biology, Faculty of Medicine, Sakarya University, Sakarya, Turkiye*

**Corresponding author: turnao@iuc.edu.tr*

Citation: Baykal Ugur A, Guney Eskiler G, Turna O (2026): Impact of histological and molecular subtype on the potential therapeutic effect of buparlisib in canine mammary gland tumours. Vet Med-Czech 71, 230–244.

Abstract: This study aims to evaluate the response of primary cells to buparlisib, a PI3K inhibitor, at varying concentrations and exposure durations across different histological and molecular subtypes of CMGTs, and to assess PI3K/Akt/mTOR pathway activity by measuring Akt and mTOR expression. Three carcinomas (C), three sarcomas (S), and two carcinosarcomas (CS) tumours were collected from the dogs. The primary cells were produced from tissues and treated with buparlisib at different doses. Subsequently, the WST-1 assay, Annexin V, and AO/PI staining were performed sequentially to evaluate the effects of buparlisib. PI3K/Akt/mTOR signalling pathway inhibition was revealed at the gene level in C, S, and CS cells following 5 μM buparlisib treatment by RT-PCR analysis. Our results demonstrated that C1 and C2 (basal-like) cells were more sensitive than C3, CS1, and CS2 cells (luminal A) upon buparlisib treatment. Liposarcoma S2 cells responded more to buparlisib than undifferentiated S cells (S1 and S3). Buparlisib also induced apoptosis and inhibited *Akt* and *mTOR* mRNA levels in C2, C3, S2 and S3 cells ($P < 0.05$). A higher rate of apoptotic cell death was observed in the C histological subtype and basal-like cells, with 62.9 ± 0.8% apoptosis in C1 and 79.1 ± 0.3% in C2. The efficacy of buparlisib was more pronounced in C2 basal-like CMGT cells and liposarcoma S2 cells with the downregulation of Akt and mTOR mRNA levels ($P < 0.001$). Therefore, PI3K inhibitors could be used to treat CMGT, particularly the basal-like molecular subtype.

Keywords: apoptosis; dog; molecular classification; PI3K/Akt/mTOR signalling pathway; tyrosin kinase inhibitors

The most common tumour types in dogs are canine mammary gland tumours (CMGT). The outcome of CMGTs is influenced by the tumour type, histologic differentiation, and several prognostic factors. CMGTs with small, well-differentiated malignant epithelial tumours may have a better

Represents the first author's PhD thesis and was supported by the Scientific and Technological Research Council of Türkiye (TUBITAK 1002, No. 121O158).

https://doi.org/10.17221/48/2025-VETMED

prognosis with a surgical approach alone, whereas undifferentiated, advanced tumours exhibit a worse prognosis and may require adjuvant therapies (Sorenmo 2003). Surgical intervention remains the primary treatment for mammary tumours, except in cases of inflammatory carcinoma and metastatic disease. Nevertheless, adjuvant and neoadjuvant therapies are also utilised as part of the treatment approach (Karayannopoulou and Lafioniatis 2016). In this context, histopathological and molecular subtype of differences play a crucial role in determining the treatment protocol for CMGT patients. Moreover, the surgical approach does not significantly affect disease-free survival and overall survival once micro- and macrometastases are formed. Chemotherapy is another treatment option, but it is often associated with side effects such as gastrointestinal toxicity, nephrotoxicity, myelotoxicity, and hepatotoxicity (Sleeckx et al. 2011). Malignant CMGTs are subdivided into carcinoma of epithelial origin, sarcoma of mesenchymal origin, and carcinosarcoma arising from both epithelial and mesenchymal tissues according to their cellular origin (Goldschmidt et al. 2011). CMGT is a heterogeneous disease that leads to different treatment responses in patients (Polyak 2011). Because of different histological and molecular features, C, CS, and S respond differently to treatment options (Lana and Dobson 2016), and thus a subtype-specific targeted therapy will contribute to future steps toward effective treatment of CMGTs. Additionally, in the treatment of CMGTs, the development of chemotherapy resistance, challenges in administering targeted therapies, different treatment responses, resistance to hormone therapy, etc., highlight the necessity for new therapeutic modalities.

The phosphoinositide 3-kinase/protein kinase B/mammalian target of rapamycin (PI3K/Akt/mTOR) pathway is the most commonly activated pathway in neoplastic processes (Agarwal et al. 2010). Overactivation of the PI3K pathway is one of the signalling abnormalities frequently observed in mammary tumours. The upregulation of phospho-Akt in the PI3K/Akt/mTOR signalling pathway, resulting from factors such as PTEN loss and mutations in the *PI3KCA* gene, contributes to alterations in the PI3K/Akt/mTOR pathway, playing a role in the progression of CMGT (Kim et al. 2021). In dogs, the frequency of mutations detected in genes associated with this pathway [phosphoinositide-3-kinase regulatory subunit 1 (*PI3KR1*), *PIK3CA*, *PTEN*, *AKT1*] has similar frequencies in human breast cancers, and thus they could be conserved across species (Vazquez et al. 2023). Therefore, this complex signalling pathway has attracted attention to developing innovative therapeutic strategies in cancer treatment (Hennessy et al. 2005).

Buparlisib (BKM120) is a potent pan-PI3K inhibitor with considerable anti-cancer properties. The antiproliferative effect and apoptotic activity of buparlisib have been revealed in various cancer types, such as breast, ovarian, lung cancer, and glioma in humans, as a result of inhibition of the PI3K pathway (Maira et al. 2012; Bertucci et al. 2023; Zhang et al. 2024). The expression of tyrosine kinase and the use of its inhibitors in CMGT cell lines have been demonstrated in various studies (Bavcar and Argyle 2012; Leis-Filho et al. 2021; Ustun-Alkan et al. 2021; Lee et al. 2024). Different histological and molecular subtypes of canine mammary tumours exhibit different signalling pathway activation and these differentially therapeutic responses to chemotherapeutic drugs due to distinct molecular characteristics (Mei et al. 2024). Therefore, the activation of the PI3K/Akt/mTOR pathway in each subtype of canine mammary tumours is important for defining targeted therapeutic strategies in veterinary oncology to determine buparlisib response. However, there are no preclinical studies evaluating the potential therapeutic effects of buparlisib on CMGTs.

To our knowledge, this is the first *in vitro* study investigating the response of CMGT primary cells to buparlisib (BKM120), a PI3K inhibitor, at varying concentrations and exposure durations across different histological and molecular subtypes of CMGTs, and assessing PI3K/Akt/mTOR pathway activity in this process. Additionally, the study presents preclinical results on the administration of buparlisib for the treatment of CMGTs.

MATERIAL AND METHOD

Tissue sampling

Ethics committee approval for using tissues collected from animals after surgery was obtained (199967 – Istanbul University Rectorate Animal Experiments Local Ethics Committee). Tissues were collected from 8 dogs. Samples included in the study were randomly selected from each his-

https://doi.org/10.17221/48/2025-VETMED

topathological group. Since non-aggressive mammary tumours can mostly be treated only surgically, cases with aggressive characteristics and requiring additional treatments were included in the study. CMGT samples were collected after mastectomy for histopathological, immunohistochemical (IHC) analysis, and primary cell cultures. The specimens were transferred to the Department of Pathology (Istanbul University-Cerrahpaşa, Faculty of Veterinary Medicine) in 10% solution of buffered formalin for histopathological and immunohistochemical analysis. Another part of the sample was placed in Roswell Park Memorial Institute (RPMI) solution and transferred to Sakarya University Faculty of Medicine, Medical Biology Department, for primary cell isolation.

Histopathological examination

Tissue samples embedded in paraffin and cut into 4–5 µm slices with a rotary microtome were stained with haematoxylin and eosin to obtain histological sections (Slaoui et al. 2017). The grading system evaluates canine mammary tumours based on three main histopathological criteria: tubule formation, nuclear pleomorphism and staining, and mitotic figure count per 10 high-power fields (HPF). The total score determines the malignancy grade, which ranges from Grade I (low malignancy) to Grade III (high malignancy). Each section was examined under a light microscope, and tumour cases were graded according to tubule formation, nuclear pleomorphism, and mitotic index ratio (Goldschmidt et al. 2011).

Based on the results, samples were diagnosed as carcinoma (C), sarcoma (S), and carcinosarcoma (CS). The cases were named C1, C2, C3; S1, S2, S3; CS1 and CS2 under the histopathological group they belonged to.

Molecular classification

Immunohistochemical staining was performed using the Mouse and Rabbit Specific HRP/DAB IHC detection Kit (Micro-polymer, ab236466; Abcam). The details of the immunohistochemical analyses are presented in Table 1. Image analysis was performed manually by two independent observers. In order to perform molecular classification, tumours were considered positive if more than 10% of tumour cells exhibited a positive reaction in oestrogen receptor (ER), progesterone receptor (PR), and HER-2 staining. For p63 staining, positivity was defined as labelling in more than 5% of tumour cells. Epithelial tumours were classified into the following subtypes: Luminal A (ER+, HER-2–), luminal B (ER+, HER-2+), basal-like (ER–, HER-2–, p63+), and normal-like (ER–, PR–, HER-2–, p63–). Accordingly, the tissues were classified as described by Im et al. (2014).

Primary cell culture isolation

Tissue samples were dissected into small pieces (3 mm to 4 mm of fragments) by a scalpel, and enzymatic disintegration was performed by adding collagenase type IV (1 mg/ml) (Sigma-Aldrich,

Table 1. Antibodies and immunohistochemical protocol parameters

Antibody	Antigen retrieval	Dilution	Primary antibody incubation	Brand	Clonality
ER	sodium citrate buffer (pH 6.0), microwave treatment at 800 W for 20 min	1 : 100	90 min at 37 °C	MyBioSource	polyclonal, rabbit
PR	sodium citrate buffer (pH 6.0), microwave treatment at 800 W for 20 min	1 : 200	90 min at 37 °C	Abcam	polyclonal, rabbit
HER2	sodium citrate buffer (pH 6.0), microwave treatment at 800 W for 20 min	1 : 100	90 min at 37 °C	MyBioSource	polyclonal, rabbit
p63	sodium citrate buffer (pH 6.0), microwave treatment at 800 W for 20 min	1 : 200	90 min at 37 °C	Santa Cruz Biotechnology	monoclonal, rabbit

ER = oestrogen receptor; HER2 = human epidermal growth factor receptor 2; PR = progesterone receptor; p63 = tumour protein 63

https://doi.org/10.17221/48/2025-VETMED

St. Louis, MO, USA) and incubated at 37 °C for 1 hour. Following, the tissue sample was further digested with trypsin-EDTA (0.25%) (Gibco; Thermo Fisher Scientific, Waltham, MA, USA) for 15 minutes. Then, the cells were centrifuged at 1 500 × *g* for 10 minutes. After centrifugation, the pellets were washed and seeded in T-25 flasks and cultured in DMEM (Gibco; Thermo Fisher Scientific, Waltham, MA, USA) medium containing 10% Foetal Bovine Serum (Gibco; Thermo Fisher Scientific, Waltham, MA, USA), 100 units/ml of penicillin-Streptomycin (Gibco; Thermo Fisher Scientific, Waltham, MA, USA), and 2 mM l-glutamine (Gibco; Thermo Fisher Scientific, Waltham, MA, USA) at 37 °C in a 5% CO_2 incubator. When the adherent cells had fully adhered to the flasks, the cells were removed and seeded for subsequent experiments.

WST-1 analysis

The cell viability was evaluated using the water-soluble tetrazolium (WST-1) kit protocol. C, S, and CS cells were seeded in 96-well plates at 2 × 10^4 cells/well and incubated overnight. Buparlisib (BKM120; Novartis Pharma AG, Basel, Switzerland) was added at different doses (0.5, 1, 2.5, 5 µM) for 24 h and 48 hours. Following treatment, WST-1 reagent (BioVision, Milpitas, CA, USA; 10 µl) was added to each well and incubated in the dark (at 37 °C for 45 minutes). An ELISA reader (Allsheng, P.R. China) was then used to measure cell viability at 450 nm. The effective concentrations and incubation time of buparlisib were determined based on the relevant literature (Yu et al. 2016; Blazquez et al. 2018). Each experiment was repeated three times. The absorbance in control cells was accepted as 100%, and cell viability after treatment with different concentrations of buparlisib was calculated as a percentage.

Assessment of the apoptotic cell death on CMGT cells

Annexin V analysis was performed to determine the apoptotic effect of buparlisib on CMGT cells. Annexin V is a calcium-dependent phospholipid-binding protein and specifically binds to phosphatidylserine. 7-AAD is a dead-cell marker used to assess cell membrane structural integrity. Therefore, early apoptotic cells were Annexin V (+) and 7-AAD (–), and late apoptotic cells were: Annexin V (+) and 7-AAD (+). CMGT cells were incubated in 6-well plates with 1 × 10^6 cells per well, and then, cells were treated with 5 µM buparlisib for 48 h according to WST-1 analysis. After treatment with buparlisib, 100 µl of Muse® Annexin V Dead stain (Millipore, Germany) was added and incubated for 30 min at room temperature in the dark. At the end of incubation, each tube was analysed on Muse™ Cell Analyser (Merck Millipore, Germany). Each experiment was repeated three times.

Assessment of the morphological changes in CMGT cells

To observe morphological changes in the cells upon treatment with buparlisib in C, S, and CS cells, acridine orange (AO) and propidium iodide (PI) staining were performed. After incubating the cells with buparlisib for 48 h, the cells were fixed with 4% PFA and stained with an AO/PI solution for 30 minutes. Finally, the cells were observed by the EVOS FL cell imaging system (Thermo Scientific, Waltham, MA, USA).

RT-PCR analysis

The inhibition of the activity of PI3K/Akt/mTOR signalling pathway by buparlisib at 5 µM for 48 h in C, S, and CS cells, and real-time polymerase chain reaction (RT-PCR) analysis was performed. After seeding into a 6-well plate with 1 × 10^6 cells per well, the cells were treated with 5 µM buparlisib for 48 hours. The Total RNA Kit (Omega Bio-Tek, Norcross, GA, USA) was used to extract total RNA from cells, and RNA quantity was measured with a Qubit 4.0 Fluorometer (Invitrogen, Carlsbad, CA, USA). The extracted RNAs were then transcribed into cDNA using the High-Capacity cDNA Reverse Transcription Kit (Thermo Fisher Scientific, Waltham, MA, USA).

TaqMan® Gene Expression Assays (Thermo Fisher Scientific, Waltham, MA, USA) primers and the corresponding TaqMan® Gene Expression Master Mix (Thermo Fisher Scientific, Waltham, MA, USA), and Step OnePlus RT-PCR (Applied

https://doi.org/10.17221/48/2025-VETMED

Biosystems, Foster city, CA, USA) system were used. β-actin (Cf04931159_m1) was selected as the endogenous reference gene, and all experiments were conducted in triplicate at a minimum. The fold change for each gene expression was normalised for each control group and for β-actin.

Statistical analysis

GraphPad Prism v6.0 was used for statistical analysis. The normality (Shapiro–Wilk) test was performed. The Mann–Whitney *U* test and Kruskal–Wallis tests were used to analyse non-parametric data.

The effect of buparlisib on cytotoxicity, apoptosis, and gene expressions in cells was analysed using the one-way analysis of variance and post-hoc Tukey test. $P < 0.05$ and $P < 0.01$ were considered statistically significant. Changes in gene expression levels were evaluated using the RT2 Profiler PCR Array Data Analysis program (https://dataanalysis.qiagen.com/pcr/arrayanalysis.php).

RESULTS

Histopathological and molecular classification of CMGTs

The study included tissues from canine mammary tumour cases that were aggressive and required additional treatments in addition to surgery. Accordingly, one lipid-rich carcinoma, one solid carcinoma, one complex carcinoma, one liposarcoma, two undifferentiated sarcomas (one with distant metastases), and two carcinosarcoma tissues were used. The molecular classification of these epithelial tissues included two basal-like and three luminal A subtypes. When individual tissue characteristics were examined, the following were observed: C1 was a tumour of atypical neoplastic cells with large cytoplasmic vacuoles and was defined as lipid-rich carcinoma (Figure 1A). C2 was a solid carcinoma composed of atypical epithelial cells organised as solid islets with areas of necrosis in their central regions (Figure 1B). C3 was a complex carcinoma (Figure 1C) in which luminal and myoepithelial cells proliferated simultaneously.

S2 was diagnosed as liposarcoma consisting of neoplastic lipocytes and lipoblasts (Figure 2A), while the histopathologic diagnosis of S1 and S3 was undifferentiated sarcoma (Figure 2B). Additionally, a distant metastasis was detected in the S1 case of the sarcoma group. CS1 and CS2 were mixed tumours containing both epithelial and mesenchymal components (Figure 2C).

According to the molecular classification determined by the IHC analysis results of the tissues, two basal-like and three luminal A tissues were identified in tissues of epithelial origin. C1 and C2 were diagnosed as basal-like, while C3 was diagnosed as luminal-A (Table 2).

In CS cases, mild ER and strong PR positivity, and negative staining for Her-2 and p63 in the epithelial components of the tumours, indicated that both tumours had luminal-A character (Figure 3). Moreover, C3 and CS1 were determined as Grade II tumours, while C1, C2, and CS2 were categorised as Grade III tumours.

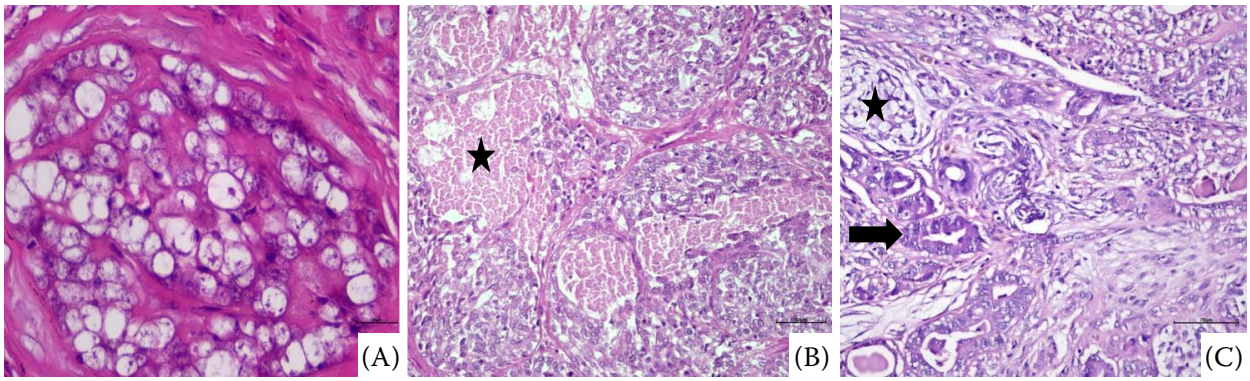

Figure 1. (A) A lipid-rich carcinoma case of large foamy vacuolated atypical epithelial cells; Bar = 20 μm. (B) Large central necrosis areas (asterisk) surrounded by neoplastic cells composing solid groups in a solid carcinoma; Bar = 70 μm. (C) A complex carcinoma case which has both luminal (arrow) and myoepithelial (asterisk) tumoral components; Bar = 70 μm. Haematoxylin & eosin

https://doi.org/10.17221/48/2025-VETMED

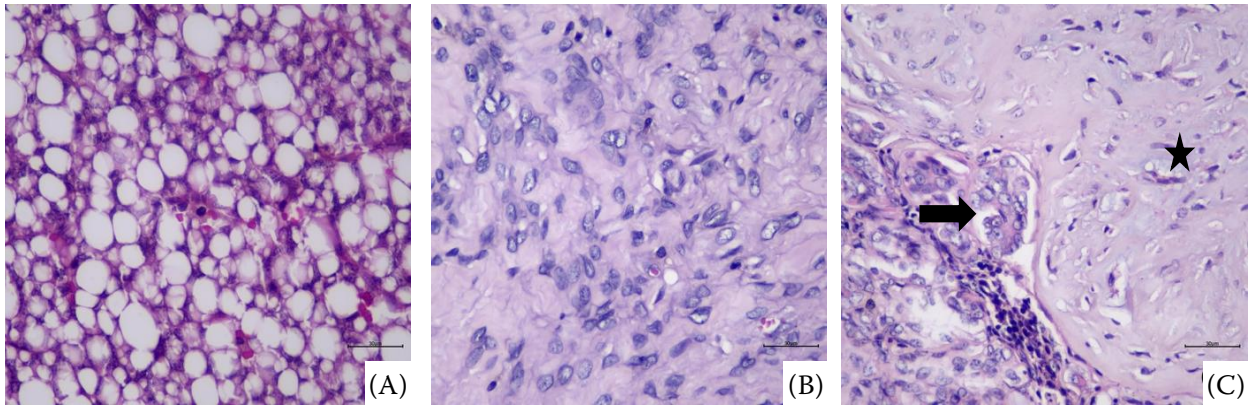

Figure 2. (A) A liposarcoma case. (B) Undifferentiated sarcoma case. (C) A carcinosarcoma case consisting of neoplastic epithelial (arrow) and mesenchymal (asterisk) components; Bar = 30 µm. Haematoxylin & eosin

Table 2. The comparison of the results of Annexin V analysis (apoptotic death) and molecular subtype with *Akt*/*mTOR* expression levels at 5 µM doses

Group	Molecular subtypes	%Total apoptotic cell death by Annexin V analysis at 5 µM	*Akt* expression levels (5 µM)	*mTOR* expression levels (5 µM)
C1	basal-like	62.9 ± 0.8%	6.53-fold ↑	8.86-fold ↑
C2	basal-like	79.1 ± 0.3%	0.16-fold ↓	0.19-fold ↓
C3	luminal A	49.4 ± 1.3%	0.97-fold ↓	0.75-fold ↓
S1	–	23 ± 0.6%	8.69-fold ↑	4.53-fold ↑
S2	–	76.9 ± 0.7%	0.10-fold ↓	0.40-fold ↓
S3	–	75 ± 0.9%	0.32-fold ↓	1.75-fold ↓
CS1	luminal A	55.6 ± 1.7%	0.50-fold ↓	0.18-fold ↓
CS2	luminal A	58.6 ± 0.8%	0.61-fold ↓	0.38-fold ↓

Akt/*mTOR* = protein kinase B/mammalian target of rapamycin; C = carcinoma; CS = carcinosarcoma; S = sarcoma

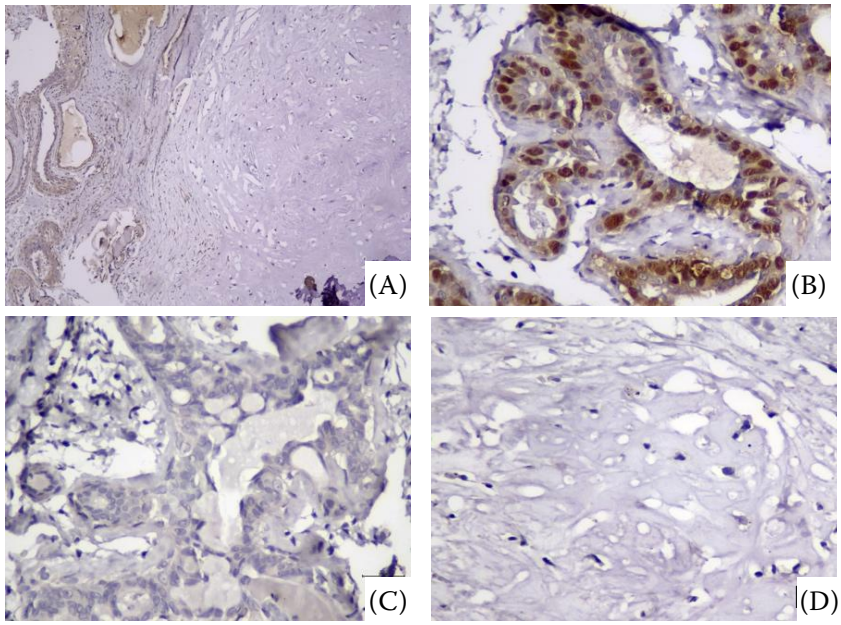

Figure 3. Carcinosarcoma case determined as luminal A in molecular subtyping
(A) Oestrogen slight positive; (B) Progesterone strong positive; (C) Her-2 negative; (D) P63 negative labelling. Bar = 100 µm (A) and 30 µm (B, C, D). Immunohistochemical staining

https://doi.org/10.17221/48/2025-VETMED

Assessment of the proliferation of CMGT cells

We analysed the viability of C, S, and CS cells at different concentrations of buparlisib using the WST-1 assay (Figure 4, Table 3). The comparison of cell viability following buparlisib treatment among groups was presented in Figure 5. After treatment with buparlisib at 1 and 5 μM for 48 h, the viability of C1 cells was 79.6 ± 3.2% and 56.3 ± 0.3%, respectively. While the proliferation rate of C2 cells was 63.5% ± 2.5 and 43.8% ± 2.4 ($P < 0.01$). Similarly, the viability of C3 cells was 69.5% ± 3.2 and 63.8% ± 2.4 at 1 and 5 μM, respectively ($P < 0.01$). In the S group, the viability of S1 cells decreased to 67.7 ± 4.0% and 75.7 ± 0.1% for 48 h at 1 and 5 μM, respectively ($P < 0.01$), whereas the proliferation of S2 cells was 55.8 ± 0.8% and 44.7 ± 0.6%, respectively. In S3 cells, cell viability decreased to 67.2 ± 3.5% and 46.5 ± 0.7% at 1 and 5 μM, respectively ($P < 0.01$). Furthermore, the viability percentages of CS1 cells treated with buparlisib 1 and 5 μM buparlisib for 48 h were 58.2 ± 4.6% and 54.3 ± 0.7%, respectively ($P < 0.01$), while the percentage of CS2 cells decreased to 53.4 ± 2.1% and 51.6 ± 0.4%, respectively ($P < 0.01$).

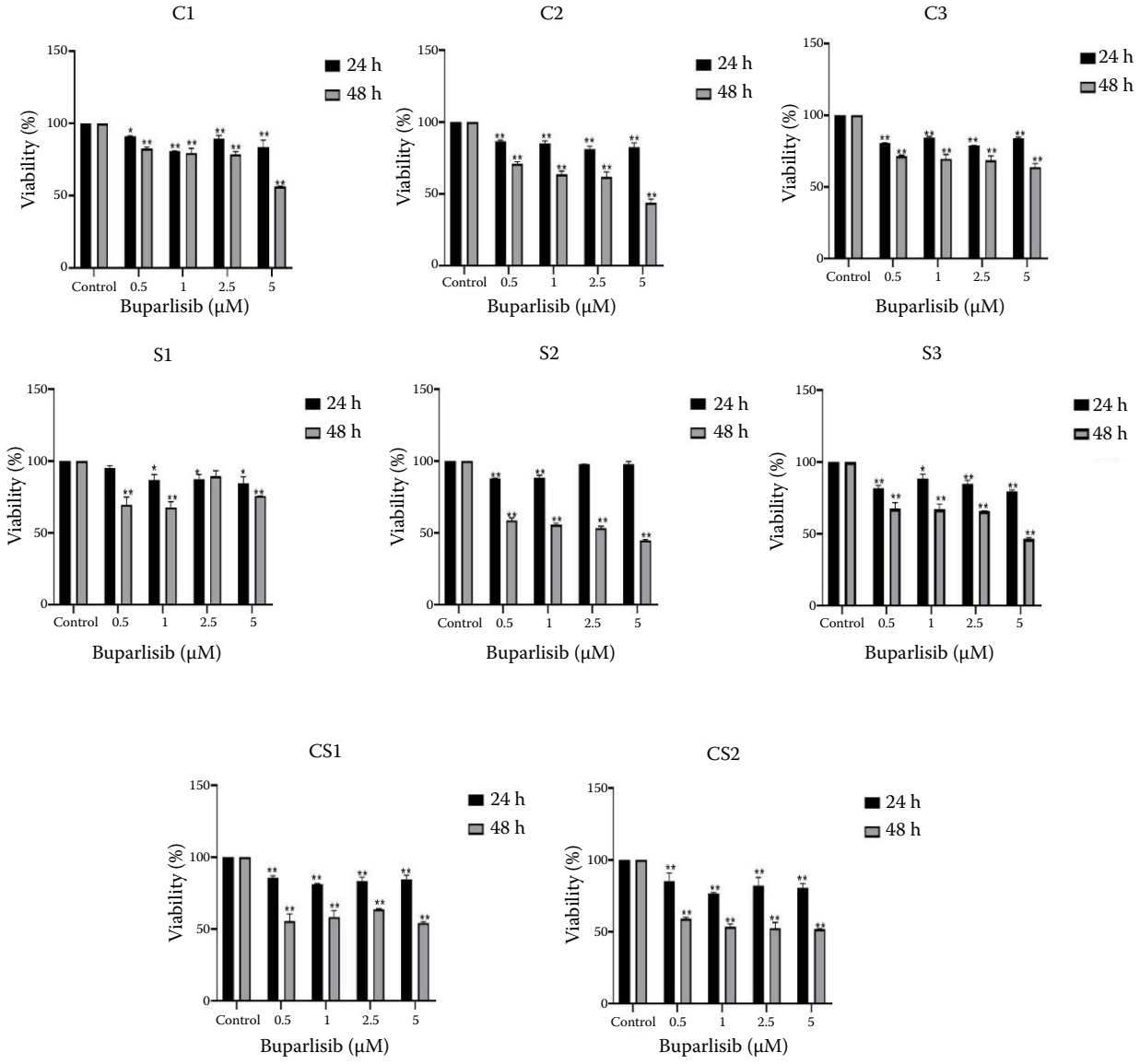

Figure 4. Determination of the cytotoxic effect of buparlisib by WST-1 analysis in C, S and CS cells for 24 and 48 h (*$P < 0.05$, **$P < 0.01$)

C = carcinoma; CS = carcinosarcoma; S = sarcoma

https://doi.org/10.17221/48/2025-VETMED

Table 3. Statistical results of ANOVA analysis

Buparlisib		C1 (*P*-value)	C2 (*P*-value)	C3 (*P*-value)	S1 (*P*-value)	S2 (*P*-value)	S3 (*P*-value)	CS1 (*P*-value)	CS2 (*P*-value)
24 h	0.5 µM	0.013 8	0.000 1	<0.000 1	0.412 4	<0.000 1	0.001	0.001 9	0.001
	1 µM	<0.000 1	<0.000 1	<0.000 1	0.006 8	<0.000 1	0.016 2	0.000 2	<0.000 1
	2.5 µM	0.004 8	<0.000 1	<0.000 1	0.01	0.342 7	0.003 4	0.000 7	0.000 2
	5 µM	0.000 3	<0.000 1	<0.000 1	0.002 7	0.316 3	0.000 5	0.001 1	0.000 1
48 h	0.5 µM	0.000 2	<0.000 1	<0.000 1	<0.000 1	<0.000 1	<0.000 1	<0.000 1	<0.000 1
	1 µM	<0.000 1	<0.000 1	<0.000 1	<0.000 1	<0.000 1	<0.000 1	<0.000 1	<0.000 1
	2.5 µM	<0.000 1	<0.000 1	<0.000 1	0.026	<0.000 1	<0.000 1	<0.000 1	<0.000 1
	5 µM	<0.000 1	<0.000 1	<0.000 1	0.000 1	<0.000 1	<0.000 1	<0.000 1	<0.000 1

These results indicated the comparison of the viability rate by WST-1 analysis in the C, S, and CS cells upon treatment with different concentrations of buparlisib for 24 and 48 h compared with the control group
C = carcinoma; CS = carcinosarcoma; S = sarcoma

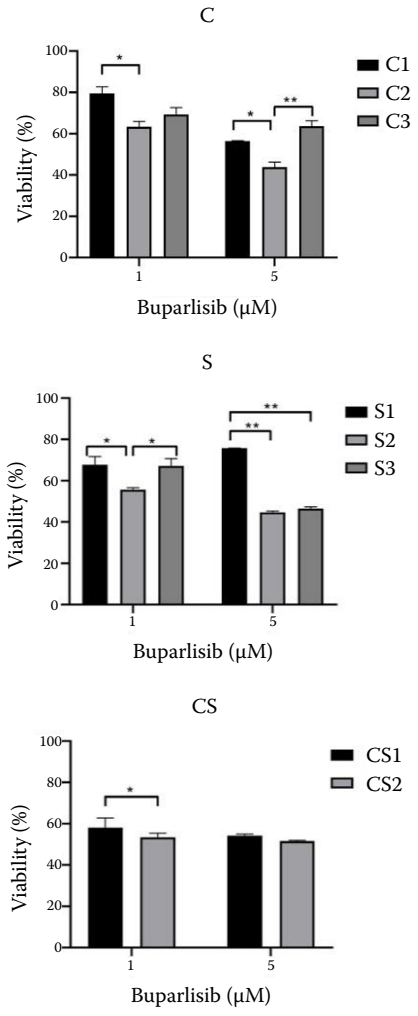

Figure 5. Comparison of buparlisib efficacy in subtypes of canine mammary gland tumour cells
C = carcinoma; CS = carcinosarcoma; S = sarcoma

Assessment of the apoptotic cell death on CMGT cells

Annexin V analysis, which shows the apoptotic effects of buparlisib on C, S, and CS cells, is shown in Figure 6 and Table 4. After 48 h treatment with 5 µM of buparlisib, the rate of total apoptotic cells significantly increased to 62.9 ± 0.8%, 79.1 ± 0.3%, and 49.4 ± 1.3% in C1, C2, and C3 cells, respectively, compared with the control ($P < 0.05$). In contrast, the rate of total apoptotic cells in S1, S2, and S3 cells treated with buparlisib at a 5 µM dose for 48 h was 23 ± 0.6%, 76.9 ± 0.7%, and 75 ± 0.9%, respectively ($P < 0.05$). In CS1 and CS2 cells treated with 5 µM buparlisib for 48 h, the percentage of total apoptotic cells was 55.6 ± 1.7% and 58.6 ± 0.8%, respectively ($P < 0.05$). The percentages of total apoptotic cell death following 1 µM and 5 µM doses of buparlisib are given in Table 2.

Assessment of the morphological changes in CMGT cells

As shown in Figure 7, apoptotic changes were observed in C, S, and CS cells after 48 h of increased buparlisib concentrations. Compared to the control group, membrane blebbing, rupture of intercellular connections, a decrease in the cell/cytoplasm ratio, and chromatin condensation were observed, especially in C, S, and CS cells treated with 5 µM buparlisib. At the indicated buparlisib concentrations, late apoptotic cells were observed in C1,

https://doi.org/10.17221/48/2025-VETMED

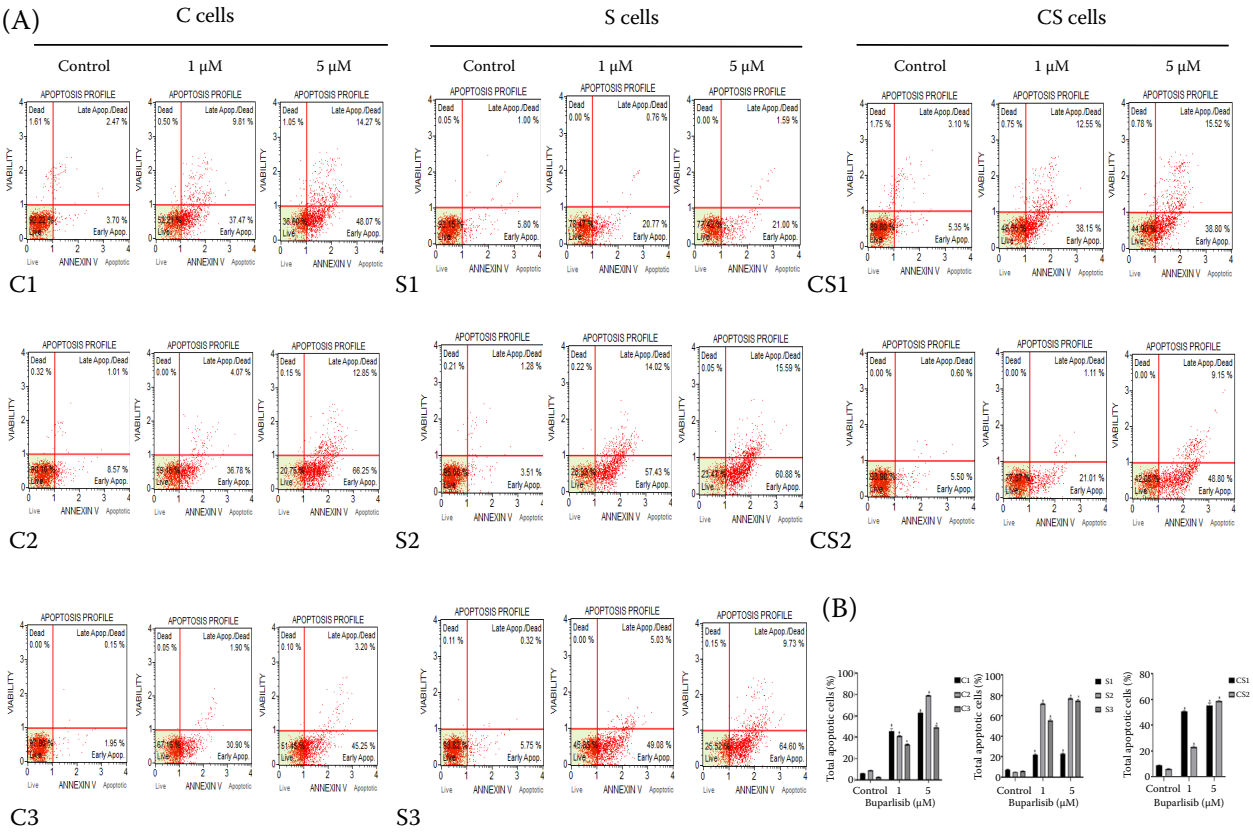

Figure 6. Determination of apoptotic effect of buparlisib on C, S and CS cells

(A) Annexin V histograms of results in C, S and CS cells following treatment with 1 and 5 μM buparlisib. (B) Statistical evaluation of total apoptotic death caused by buparlisib compared to control group (*$P < 0.05$, **$P < 0.01$)

C = carcinoma; CS = carcinosarcoma; S = sarcoma

Table 4. Statistical results of ANOVA analysis

Buparlisib		C1	C2	C3	S1	S2	S3	CS1	CS2
		(*P*-value)	(*P*-value)	(*P*-value)	(*P*-value)	(*P*-value)	(*P*-value)	(*P*-value)	(*P*-value)
48 h	1 μM	0.039 6	0.021 1	0.021 1	0.021 1	0.021 1	0.021 2	0.021 1	0.025 8
	5 μM	0.021 1	0.021 1	0.021 1	0.021 1	0.021 1	0.021 1	0.021 3	0.021 1
	1 μM~5 μM	0.125 2	0.021 1	0.031 4	0.034	0.021 5	0.085 7	0.183 5	0.021 1

These results indicated the comparison of the apoptotic rate by Annexin V analysis in the C, S, and CS cells upon treatment with different concentrations (1 and 5 μM) of buparlisib for 48 h compared with the control group

C = carcinoma; CS = carcinosarcoma; S = sarcoma

C2, and C3 cells. More cytoplasmic vacuoles, cell membrane blebbing, and nuclear damage were observed in S1, S2, and S3 cells, especially at 5 μM buparlisib compared to 1 μM buparlisib. It was also found that buparlisib induced more apoptosis in S2 and S3 cells than in S1 cells. In CS1 and CS2 cells, buparlisib caused especially many cytoplasmic vacuoles and nuclear damage. Our results were generally correlated with Annexin V analysis findings overall and consistently.

Assessment of the effect of buparlisib on the *PI3K*/*Akt*/*mTOR* signalling pathway at the gene level

The mRNA levels of *Akt* and *mTOR* in C, S, and CS cells were evaluated by RT-PCR after treatment with 5 μM buparlisib for 48 h, the most effective dose and incubation time; the results are shown in Figure 8.

Akt expression levels were 6.53-, 0.16-, and 0.97-fold, and *mTOR* levels were determined as 8.86-,

https://doi.org/10.17221/48/2025-VETMED

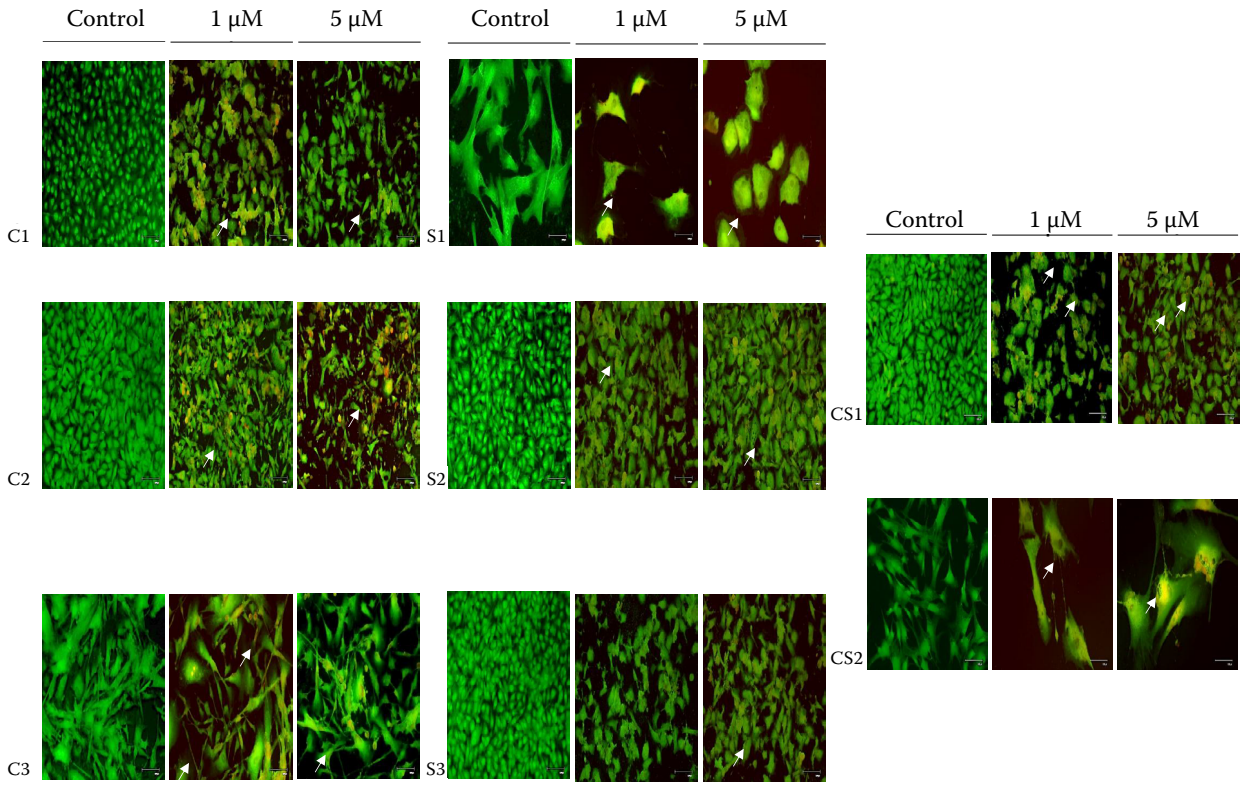

Figure 7. Visualisation of morphological changes in canine mammary gland tumour cells treated with buparlisib at 1 and 5 μM concentration for 48 h (scale bar: 100 μm)

C = carcinoma; CS = carcinosarcoma; S = sarcoma

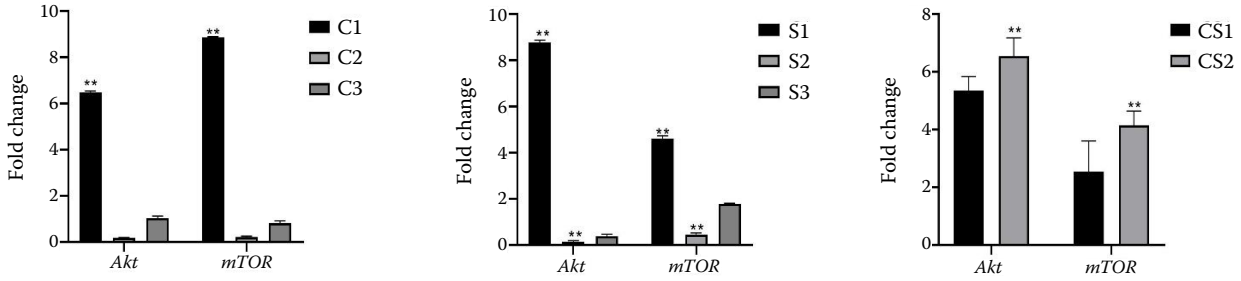

Figure 8. Evaluation of the effect of buparlisib on the *PI3K*/*Akt*/*mTOR* signalling pathway at the gene level in C, S and CS cells at a concentration of 5 μM for 48 h (*$P < 0.05$, **$P < 0.01$)

C = carcinoma; CS = carcinosarcoma; *PI3K*/*Akt*/*mTOR* = phosphoinositide 3-kinase/protein kinase B/mammalian target of rapamycin; S = sarcoma

0.19-, and 0.75-fold in C1, C2, and C3 cells, respectively, compared to the control group. Therefore, *Akt* and *mTOR* expression levels were significantly upregulated in C1 cells despite the 5 μM buparlisib treatment ($P < 0.01$).

Akt mRNA expression levels were 8.69-, 0.10-, and 0.32-fold, and *mTOR* expression levels were 4.53-, 0.40-, and 1.75-fold in S1, S2, and S3 cells, respectively, compared to the control group. Although *Akt* and *mTOR* expression levels were significantly upregulated in S1 cells compared to the control group, their expression levels were significantly downregulated in S2 cells after buparlisib treatment ($P < 0.01$).

In CS1 and CS2 cells, *Akt* mRNA expression levels were 0.50- and 0.61-fold, and *mTOR* expression levels were 0.18- and 0.38-fold, respectively, following treatment with buparlisib. Therefore, *Akt* and *mTOR* expression levels were significantly

https://doi.org/10.17221/48/2025-VETMED

downregulated in CS1 and CS2 cells compared to the control group after 5 μM buparlisib treatment ($P < 0.01$). Furthermore, we compared the total apoptotic death rate with *Akt* and *mTOR* expression levels at 5 μM concentrations in C, S, and CS cells (Table 2). As shown in Table 2, *Akt* and *mTOR* mRNA levels were downregulated in the luminal A subtype following buparlisib treatment. However, the basal-like subtypes responded differently to buparlisib. More apoptotic cell death was analysed in C2 cells than in C1 cells due to lower expression of both *Akt* and *mTOR* by buparlisib. Additionally, buparlisib downregulated *Akt* and *mTOR* more effectively in S2 and S3 cells, inducing apoptotic cell death. Therefore, the response of C, S, and CS cells to buparlisib was different due to the differential expression level of *Akt* and *mTOR* after treatment with buparlisib. Additionally, *Akt* and *mTOR* expression levels were downregulated in luminal A CS1 and CS2 cells following buparlisib treatment. However, the expression levels were different in basal-like C1 and C2 cells upon buparlisib. Therefore, molecular and histological subtype, tumour heterogeneity, and mutation profile could regulate these gene expression levels.

DISCUSSION

Histopathological differentiation of an epithelial mammary gland tumour determines its biological behaviour and influences prognosis, which worsens with loss of differentiation. Considering this differentiation in the WHO (The World Health Organisation) Histological Classification System, malignancy increases from non-infiltrating carcinoma (carcinoma *in situ*) to complex carcinoma (two cell types), simple carcinoma (one cell type), tubulopapillary type, solid type, and anaplastic carcinoma (Misdorp et al. 1999). Another type defined in the CMGT classification is the special type of malignant epithelial tumour, which tends to spread to other parts of the body (Goldschmidt et al. 2011). Lipid-rich cell carcinoma is a special type of CMGT that is extremely aggressive with high metastasis rates and poor prognosis (Perossi et al. 2020). Sarcoma and carcinosarcoma are types of CMGT that have a strong tendency to metastasize and are known for their poor prognosis (Sorenmo 2003). Tumour types with different aggressive characteristics and those that cannot be treated with operative treatment alone and require additional treatments were included in the study. In the current study, the response of CMGT primary cells to buparlisib and the activity of the PI3K/Akt/mTOR pathway were evaluated for the first time. Our *in vitro* findings demonstrated that buparlisib significantly inhibited CMGT cell proliferation via apoptosis. In particular, C cells were more responsive to buparlisib due to the basal-like subtype. Additionally, liposarcoma S cells were more sensitive to buparlisib than undifferentiated S cells, as evidenced by lower *Akt* and *mTOR* mRNA levels after treatment. Therefore, histological and molecular subtypes could affect the response to buparlisib. Yeom et al. (2023) state that alpelisib, as a tyrosine kinase inhibitor, induces a higher cytotoxic effect in the C histologic subtype of CMGT harbouring the *PIK3CA* mutation. In another study, alpelisib exhibits antiproliferative efficacy by suppressing the activation of the PI3K/Akt signalling pathway in CMGT tumour cells with *PIK3CA* mutations (Park et al. 2024). These findings suggest that *PIK3CA* mutation may contribute to the favourable therapeutic response to PI3K inhibitors. Therefore, further investigations should be required for the effects of *PI3KCA* mutation in the response to buparlisib in C basal-like subtypes. Additionally, the molecular mechanisms behind the apoptotic death by buparlisib should be further investigated at gene and protein levels, as well as transcriptomic analysis, to identify the activation of intrinsic or extrinsic pathways of apoptosis (Liu et al. 2013; Mariotti et al. 2017). In accordance with a previous study (Yoo et al. 2023) reporting that palmatine induces apoptosis in carcinoma cell lines, our findings revealed that buparlisib also triggered apoptosis in the C group. The pronounced increase in late apoptotic cells indicates that buparlisib activates apoptotic signalling and effectively inhibits the PI3K/Akt/mTOR pathway. Furthermore, we observed cytoplasmic vacuoles in the C and CS cell groups. Buparlisib may induce autophagy in the cells (Kelekar 2006). Therefore, further investigation associated with autophagy biomarkers, including Atg, Beclin-1, p62, and LC3 protein levels, etc., is required to assess the autophagic effects of buparlisib in the CMGT cells. An understanding of the potential role in buparlisib-induced autophagy could provide insight into its dual regulation of cell survival and death and provide new insight into the development of improved targeted therapies.

https://doi.org/10.17221/48/2025-VETMED

The PI3K/Akt/mTOR pathway is studied to be the most commonly activated pathway in oncogenesis (Agarwal et al. 2010). It has been reported that PI3K inhibitors suppress the abnormal activation of the PI3K/Akt/mTOR signalling pathway in different cancer cells. However, the effect of these inhibitors varies depending on the cell type (Chen et al. 2012; Campos et al. 2014). Campos et al. (2014) demonstrated that the Akt/mTOR pathway plays a notable role in the pathogenesis of thyroid carcinoma cases in dogs. Although the overactivation of the PI3K/Akt/mTOR pathway and the effect of specific PI3K inhibitors have been assessed in different human cancer types and some canine tumours, there is no study evaluating the activity of this signalling pathway in different histological and molecular subtypes of CMGT. In our study, the molecular and histological subtype of CMGT could affect the buparlisib response.

Notably, the inhibition of the PI3K/Akt/mTOR signalling pathway has been evaluated in human liposarcoma cells or cases. Guo et al. (2014) state that PI-103, as an inhibitor, induces apoptosis by inhibiting PI3K/Akt activation in the liposarcoma cell line. In canine liposarcoma cases, Avallone et al. (2017) investigated the expression of tyrosine kinase receptors and the involvement of these receptors associated with neoplastic cell proliferation. In our study, we have investigated the effects of buparlisib on liposarcoma CMGT cells. The findings indicated that the S2 (liposarcoma) cell group responded more to buparlisib. Additionally, buparlisib did not effectively suppress the signalling pathway in undifferentiated S1 cells, unlike S3 cells. The different responses of S1 and S3 cells to buparlisib are considered to be due to the activation of an alternative signalling pathway associated with metastasis. In addition to the metastatic effect, the greater sensitivity of S2 cells to buparlisib may be associated with lipid metabolism, as buparlisib exerts its effect by competitively binding to the lipid kinase domain of ATP (Xing et al. 2021).

Basal-like tumours, which do not express hormone receptors (ER, PR) or HER-2, have a poor prognosis with different clinical outcomes. Histologically, these tumours are characterised by a high grade and mitotic index (Carey et al. 2006). Triple-negative tumours share phenotypic characteristics with basal-like mammary tumours (Pala et al. 2012). In this study, the C1 and C2 cases were molecularly diagnosed as basal-like. The C1 and C2 cases also had triple-negative characteristics. The C3 tumour was classified as luminal A. Following buparlisib treatment, the viability of C1 and C2 cells decreased more than that of C3 cells. In human breast cancer, breast tumours with a basal-like molecular subtype exhibit an aberrant activation in the PI3K/Akt pathway. Additionally, triple-negative tumours demonstrate greater sensitivity than the luminal A subtype (Valentin et al. 2012; Meuten et al. 2024). PI3K mutations and PTEN loss are commonly observed in human cases of triple-negative breast tumours. In this context, the use of buparlisib, a PI3K inhibitor, either as a monotherapy or in combination, could be considered as novel treatment strategies of CMGT (Solzak et al. 2017; Pascual and Turner 2019; Garrido-Castro et al. 2020). The presented study demonstrated the efficacy of buparlisib in triple-negative basal-like C tumours, and our results were consistent with the studies conducted in humans.

Furthermore, the hyperactivation of the PI3K/Akt/mTOR signalling pathway plays a role in the oncogenesis of ER+ tumours. The frequency of alterations in this signalling pathway suggests that PI3K signalling is crucial in the development of ER+ mammary tumours (Ciruelos Gil 2014). In this study, the downregulation in the PI3K/Akt/mTOR pathway was observed in CS groups following buparlisib treatment. Buparlisib was more effective in CS2 cells than CS1 cells; both were luminal A subtypes. This difference could be related to the different scores of ER expression levels. The HER-2 receptor also plays a role in activating this signalling pathway. The overexpression or amplification of HER-2 stimulates tumour growth, invasiveness, and aggressiveness by activating various signalling cascades, such as the PI3K/Akt pathways. In line with previous studies (Leis-Filho et al. 2021) showing that lapatinib inhibits the proliferation of HER-2 negative cells such as UNESP-MM1 through alternative pathways, our findings demonstrated that buparlisib suppressed the proliferation of HER-2 negative canine mammary carcinoma cells via the inhibition of PI3K/Akt/mTOR pathway.

Additionally, PI3K activation plays a critical role in oncogenesis and is involved in developing resistance to therapy in ER+/HER-2+ tumours (Ortega et al. 2020). Therefore, HER-2 phosphorylation could lead to the PI3K/Akt/mTOR pathway activation. However, further investigations should

https://doi.org/10.17221/48/2025-VETMED

be performed for especially HER2+ and/or luminal B molecular subtype of CMGTs.

However, our study had some limitations. Firstly, further studies should be conducted on the PI3K/Akt/mTOR signalling pathway inhibition by different inhibitors in preclinical studies. Additionally, the effects of buparlisib on healthy mammary cells could be analysed. Thirdly, different responses to buparlisib could be mediated by genetic alterations in the *PI3KCA* gene, especially in histologic or molecular subtypes of CMGT tumours. Therefore, genomic and transcriptomic analysis could be performed to assess the association of genetic alterations with buparlisib response. Finally, the changes in *Akt* and *mTOR* levels could not be correlated with the protein level of *Akt* and *mTOR* due to the activity of post-transcriptional mechanisms involved in the conversion of mRNA to protein (Szallasi 1999; Baldi and Long 2001). Therefore, further molecular analysis, including western blot, could be performed to verify the suppression of this signalling pathway by buparlisib. More comprehensive *in vitro* and *in vivo* studies should be performed to evaluate the therapeutic potential and safety profile of buparlisib in the treatment of CMGT. Preclinical studies would provide critical insights into its clinical applicability and translational relevance in veterinary oncology.

In the current study, our results suggest that buparlisib could be considered an innovative therapeutic approach for treating CMGT tumours, and that histological and molecular classifications could affect buparlisib's response. Among them, triple-negative C and liposarcoma S cells were susceptible to buparlisib. These findings suggest that buparlisib may serve as a promising therapeutic candidate for canine mammary gland tumours by targeting the PI3K/Akt/mTOR pathway. Therefore, preclinical results on the therapeutic potential of buparlisib may provide new insights for further studies using more comprehensive tumour samples in veterinary oncology, particularly for aggressive or treatment-resistant tumour types.

Acknowledgement

The authors gratefully acknowledge Prof. Dr. Funda Yildirim and Dr. Damla Haktanir for their expert contributions to the histopathological and IHC analysis conducted as part of this study.

Conflicts of interest

The authors declare no conflict of interest.

REFERENCES

Agarwal R, Carey M, Hennessy B, Mills GB. PI3K pathway-directed therapeutic strategies in cancer. Curr Opin Investig Drugs. 2010 Jun;11(6):615-28.

Avallone G, Pellegrino V, Roccabianca P, Lepri E, Crippa L, Beha G, De Tolla L, Sarli G. Tyrosine kinase receptor expression in canine liposarcoma. Vet Pathol. 2017 Mar; 54(2):212-7.

Baldi P, Long AD. A Bayesian framework for the analysis of microarray expression data: Regularized t-test and statistical inferences of gene changes. Bioinformatics. 2001 Jun;17(6):509-19.

Bavcar S, Argyle DJ. Receptor tyrosine kinase inhibitors: Molecularly targeted drugs for veterinary cancer therapy. Vet Comp Oncol. 2012 Sep;10(3):163-73.

Bertucci A, Bertucci F, Goncalves A. Phosphoinositide 3-kinase (PI3K) inhibitors and breast cancer: An overview of current achievements. Cancers (Basel). 2023 Feb 23; 15(5):1416.

Blazquez R, Wlochowitz D, Wolff A, Seitz S, Wachter A, Perera-Bel J, Bleckmann A, Beissbarth T, Salinas G, Riemenschneider MJ, Proescholdt M, Evert M, Utpatel K, Siam L, Schatlo B, Balkenhol M, Stadelmann C, Schildhaus HU, Korf U, Reinz E, Wiemann S, Vollmer E, Schulz M, Ritter U, Hanisch UK, Pukrop T. PI3K: A master regulator of brain metastasis-promoting macrophages/microglia. Glia. 2018 Nov;66(11):2438-55.

Campos M, Kool MM, Daminet S, Ducatelle R, Rutteman G, Kooistra HS, Galac S, Mol JA. Upregulation of the PI3K/Akt pathway in the tumorigenesis of canine thyroid carcinoma. J Vet Intern Med. 2014 Nov-Dec;28(6):1814-23.

Carey LA, Perou CM, Livasy CA, Dressler LG, Cowan D, Conway K, Karaca G, Troester MA, Tse CK, Edmiston S, Deming SL, Geradts J, Cheang MC, Nielsen TO, Moorman PG, Earp HS, Millikan RC. Race, breast cancer subtypes, and survival in the Carolina Breast Cancer Study. JAMA. 2006 Jun 7;295(21):2492-502.

Chen YT, Tan KA, Pang LY, Argyle DJ. The class I PI3K/Akt pathway is critical for cancer cell survival in dogs and offers an opportunity for therapeutic intervention. BMC Vet Res. 2012 May 30;8:73.

Garrido-Castro AC, Saura C, Barroso-Sousa R, Guo H, Ciruelos E, Bermejo B, Gavila J, Serra V, Prat A, Pare L, Celiz P, Villagrasa P, Li Y, Savoie J, Xu Z, Arteaga CL, Krop IE, Solit DB, Mills GB, Cantley LC, Winer EP, Lin NU,

https://doi.org/10.17221/48/2025-VETMED

Rodon J. Phase 2 study of buparlisib (BKM120), a pan-class I PI3K inhibitor, in patients with metastatic triple-negative breast cancer. Breast Cancer Res. 2020 Nov 2; 22(1):120.

Ciruelos Gil EM. Targeting the PI3K/AKT/mTOR pathway in estrogen receptor-positive breast cancer. Cancer Treat Rev. 2014 Aug;40(7):862-71.

Goldschmidt M, Pena L, Rasotto R, Zappulli V. Classification and grading of canine mammary tumors. Vet Pathol. 2011 Jan;48(1):117-31.

Guo S, Lopez-Marquez H, Fan KC, Choy E, Cote G, Harmon D, Nielsen GP, Yang C, Zhang C, Mankin H, Hornicek FJ, Borger DR, Duan Z. Synergistic effects of targeted PI3K signaling inhibition and chemotherapy in liposarcoma. PLoS One. 2014 Apr 2;9(4):e93996.

Hennessy BT, Smith DL, Ram PT, Lu Y, Mills GB. Exploiting the PI3K/AKT pathway for cancer drug discovery. Nat Rev Drug Discov. 2005 Dec;4(12):988-1004.

Im KS, Kim NH, Lim HY, Kim HW, Shin JI, Sur JH. Analysis of a new histological and molecular-based classification of canine mammary neoplasia. Vet Pathol. 2014 May; 51(3):549-59.

Karayannopoulou M, Lafioniatis S. Recent advances on canine mammary cancer chemotherapy: A review of studies from 2000 to date. Rev Med Vet. 2016 Oct;167(7-8): 192-200.

Kelekar A. Autophagy. Ann N Y Acad Sci. 2006 Dec;1066: 259-71.

Kim SH, Seung BJ, Cho SH, Lim HY, Bae MK, Sur JH. Dysregulation of PI3K/Akt/PTEN pathway in canine mammary tumor. Animals (Basel). 2021 Jul 12;11(7):2079.

Lana SE, Dobson JM. Principles of chemotherapy. In: Dobson JM, Lascelles BDX, editors. Manual of canine and feline oncology. Gloucester: British Small Animal Veterinary Association; 2016. p. 59-79.

Lee HG, Lim GH, An JH, Park SM, Seo KW, Youn HY. In vitro evaluation of the antitumor activity of axitinib in canine mammary gland tumor cell lines. J Vet Sci. 2024 Jan;25(1):e1.

Leis-Filho AF, de Faria Lainetti P, Emiko Kobayashi P, Fonseca-Alves CE, Laufer-Amorim R. Effects of lapatinib on HER2-positive and HER2-negative canine mammary carcinoma cells cultured in vitro. Pharmaceutics. 2021 Jun 17;13(6):897.

Liu JL, Chang KC, Lo CC, Chu PY, Liu CH. Expression of autophagy-related protein Beclin-1 in malignant canine mammary tumors. BMC Vet Res. 2013 Apr 11;9:75.

Maira SM, Pecchi S, Huang A, Burger M, Knapp M, Sterker D, Schnell C, Guthy D, Nagel T, Wiesmann M, Brachmann S, Fritsch C, Dorsch M, Chene P, Shoemaker K, De Pover A, Menezes D, Martiny-Baron G, Fabbro D, Wilson CJ, Schlegel R, Hofmann F, Garcia-Echeverria C, Sellers WR, Voliva CF. Identification and characterization of NVP-BKM120, an orally available pan-class I PI3-kinase inhibitor. Mol Cancer Ther. 2012 Feb;11(2):317-28.

Mariotti F, Mari S, Magi GE. Immunohistochemical evaluation of p62 in canine mammary tumours. J Comp Pathol. 2017 Jan;156(1):121.

Mei C, Liu Y, Liu Z, Zhi Y, Jiang Z, Lyu X, Wang H. Dysregulated signaling pathways in canine mammary tumor and human triple negative breast cancer: Advances and potential therapeutic targets. Int J Mol Sci. 2024 Dec 27; 26(1):145.

Meuten TK, Dean GA, Thamm DH. Review: The PI3K-AKT-mTOR signal transduction pathway in canine cancer. Vet Pathol. 2024 May;61(3):339-56.

Misdorp W, Else RW, Hellmen E, Lipscomb TP. Histological classification of mammary tumors of the dog and the cat. 2nd series, vol. 7. Washington (DC): Armed Forces Institute of Pathology, American Registry of Pathology, World Health Organization; 1999. 58 p.

Ortega MA, Fraile-Martinez O, Asunsolo A, Bujan J, Garcia-Honduvilla N, Coca S. Signal transduction pathways in breast cancer: The important role of PI3K/Akt/mTOR. J Oncol. 2020 Mar 9;2020:9258396.

Pala EE, Bayol U, Cumurcu S, Keskin E. Triple-negatif/bazal benzeri meme kanserinin immunohistokimyasal ozellikleri [Immunohistochemical characteristics of triple negative/basal-like breast cancer]. Turk Patoloji Derg. 2012;28(3):238-44. Turkish.

Park SY, Baek YB, Lee CH, Kim HJ, Kim HP, Jeon YJ, Song JE, Jung SB, Kim HJ, Moon KS, Park SI, Lee CM, Kim SH. Establishment of canine mammary gland tumor cell lines harboring PI3K/Akt activation as a therapeutic target. BMC Vet Res. 2024 May 29;20(1):233.

Pascual J, Turner NC. Targeting the PI3-kinase pathway in triple-negative breast cancer. Ann Oncol. 2019 Jul 1; 30(7):1051-60.

Perossi IFS, Martinelli PEB, Bonato L, Lima GP, Bertolo PHL, Costa RRME, Gomez JLA, De Nardi AB, Vasconcelos RO. Lipid rich carcinoma in canine mammary gland with metastasis in the abdominal cavity. Braz J Vet Pathol. 2020;13(1):26-32.

Polyak K. Heterogeneity in breast cancer. J Clin Invest. 2011 Oct;121(10):3786-8.

Slaoui M, Bauchet AL, Fiette L. Tissue sampling and processing for histopathology evaluation. Methods Mol Biol. 2017;1641:101-14.

Sleeckx N, de Rooster H, Veldhuis Kroeze EJ, Van Ginneken C, Van Brantegem L. Canine mammary tumours, an overview. Reprod Domest Anim. 2011 Dec;46(6): 1112-31.

https://doi.org/10.17221/48/2025-VETMED

Solzak JP, Atale RV, Hancock BA, Sinn AL, Pollok KE, Jones DR, Radovich M. Dual PI3K and Wnt pathway inhibition is a synergistic combination against triple negative breast cancer. NPJ Breast Cancer. 2017 Apr 26;3:17.

Sorenmo K. Canine mammary gland tumors. Vet Clin North Am Small Anim Pract. 2003 May;33(3):573-96.

Szallasi Z. Genetic network analysis in light of massively parallel biological data acquisition. Pac Symp Biocomput. 1999:5-16.

Ustun-Alkan F, Bakirel T, Ustuner O, Anlas C, Cinar S, Yildirim F, Gurel A. Effects of tyrosine kinase inhibitor-masitinib mesylate on canine mammary tumour cell lines. J Vet Res. 2021 Jul 24;65(3):351-9.

Valentin MD, da Silva SD, Privat M, Alaoui-Jamali M, Bignon YJ. Molecular insights on basal-like breast cancer. Breast Cancer Res Treat. 2012 Jul;134(1):21-30.

Vazquez E, Lipovka Y, Cervantes-Arias A, Garibay-Escobar A, Haby MM, Queiroga FL, Velazquez C. Canine mammary cancer: State of the art and future perspectives. Animals (Basel). 2023 Oct 9;13(19):3147.

Xing J, Yang J, Gu Y, Yi J. Research update on the anticancer effects of buparlisib. Oncol Lett. 2021 Apr;21(4):266.

Yeom J, Cho Y, Ahn S, Jeung S. Anticancer effects of alpelisib on PIK3CA-mutated canine mammary tumor cell lines. Front Vet Sci. 2023 Nov 15;10:1279535.

Yoo MJ, Choi J, Jang YJ, Park SY, Seol JW. Anti-cancer effect of palmatine through inhibition of the PI3K/AKT pathway in canine mammary gland tumor CMT-U27 cells. BMC Vet Res. 2023 Oct 25;19(1):223.

Yu F, Zhao J, Hu Y, Zhou Y, Guo R, Bai J, Zhang S, Zhang H, Zhang J. The combination of NVP-BKM120 with trastuzumab or RAD001 synergistically inhibits the growth of breast cancer stem cells in vivo. Oncol Rep. 2016 Jul; 36(1):356-64.

Zhang HP, Jiang RY, Zhu JY, Sun KN, Huang Y, Zhou HH, Zheng YB, Wang XJ. PI3K/AKT/mTOR signaling pathway: An important driver and therapeutic target in triple-negative breast cancer. Breast Cancer. 2024 Jul;31(4): 539-51.

Received: July 1, 2025
Accepted: February 24, 2026
Published online: June 29, 2026